

# Atmospheric depositional fluxes of cosmogenic $^{32}\text{P}$ , $^{33}\text{P}$ and $^7\text{Be}$ in the Sevastopol region

I. I. Dovhyi<sup>1</sup> · D. A. Kremenchutskii<sup>1</sup> · V. Yu. Proskurnin<sup>2</sup> · O. N. Kozlovskaya<sup>1</sup>

Received: 13 June 2017 / Published online: 31 October 2017  
© Akadémiai Kiadó, Budapest, Hungary 2017

**Abstract** Depositional fluxes of  $^{32}\text{P}$ ,  $^{33}\text{P}$  and  $^7\text{Be}$  with atmospheric precipitations were studied in the Sevastopol region in the period from January 2016 through December 2016. It was shown that the average specific activity was 2.53 dpm L<sup>-1</sup> for  $^{33}\text{P}$ , 2.29 dpm L<sup>-1</sup> for  $^{32}\text{P}$ , and 240.5 dpm L<sup>-1</sup> for  $^7\text{Be}$ . The average radionuclide fluxes in individual rainfall events were 12.51 and 13.95 dpm m<sup>-2</sup> day<sup>-1</sup> for  $^{32}\text{P}$  and  $^{33}\text{P}$ , respectively, the average ratio of  $^{33}\text{P}/^{32}\text{P}$  being 1.11. The average flux of  $^7\text{Be}$  was 1177 dpm m<sup>-2</sup> day<sup>-1</sup>. Using flux relationships of  $^{32}\text{P}$  versus  $^7\text{Be}$  and  $^{33}\text{P}$  versus  $^7\text{Be}$  monthly and annual flux values of  $^{32}\text{P}$  and  $^{33}\text{P}$  with atmospheric precipitations were calculated.

**Keywords**  $^{32}\text{P}$  ·  $^{33}\text{P}$  ·  $^7\text{Be}$  · Cosmogenic radionuclides · Atmospheric depositions

## Introduction

Short-lived isotopes of  $^{32}\text{P}$  and  $^{33}\text{P}$  were discovered in rain water over 60 years ago [1, 2] and used to study processes in the ocean and the atmosphere [3].  $^{32}\text{P}$ ,  $^{33}\text{P}$  produced in the atmosphere as a result of Ar-spallations [4].

Phosphorus is a vital element for energy and growth in all living organisms. The  $\beta$ -emitting short-lived cosmogenic isotopes of  $^{32}\text{P}$  ( $T_{1/2} = 25.3$  days,  $E_{\max} = 1.71$  MeV) and  $^{33}\text{P}$  ( $T_{1/2} = 14.3$  days,  $E_{\max} = 0.249$  MeV) were widely used for studying the biogeochemical phosphorus cycle in the ocean [5, 6].

The relatively short-lived radionuclides such as  $^{32}\text{P}$ ,  $^{33}\text{P}$  are most useful for study numerous processes at short time scales.  $^{32}\text{P}$  and  $^{33}\text{P}$  were used as important tracers to study processes in the atmosphere: the circulation in the stratosphere [7], the vertical structure of the troposphere [8], stratosphere/troposphere exchange [9], and as ozone tracers [10]. The  $^{32}\text{P}$  and  $^{33}\text{P}$  tracers were all the more important in marine research for surface layer biodynamic studies [3, 11].

Recent studies [12, 13] performed with the  $^{33}\text{P}$  radio-tracer demonstrated that phosphonates could play the key role in the biogeochemical cycle of phosphorus in the ocean. To date some aspects of the phosphorus cycle in the Black Sea region were poorly studied: the concentration of various organophosphorus compounds, the turnover rate and turnover time, the uptake of  $^{33}\text{P}$  by phosphate or adenosinetriphosphate were unknown. The  $^{32}\text{P}$  and  $^{33}\text{P}$  atmospheric deposition fluxes data were necessary for modeling their behavior in the ocean.

As  $^{32}\text{P}$  and  $^{33}\text{P}$  concentrations in sea water are three orders of magnitude lower than the ones in rainwater, for a long time there was no method developed for concentrating the above radionuclides. For the first time, it was done in the pioneering works of Lal et al. [14–17]. Later, improved methods for the isolation and concentration of  $^{32}\text{P}$  and  $^{33}\text{P}$  were proposed: in the works of Waser et al. [18–21] concentration of  $^{32}\text{P}$  and  $^{33}\text{P}$  from rainwater samples on alumina, purification of it by the double precipitation of  $(\text{NH}_4)_3[\text{PMo}_{12}\text{O}_{40}] \cdot 2\text{H}_2\text{O}$  and precipitation of

D. A. Kremenchutskii, V. Yu. Proskurnin, and O. N. Kozlovskaya:  
Co-authors

✉ I. I. Dovhyi  
dovhyi.illarion@yandex.ru

<sup>1</sup> Marine Hydrophysical Institute of RAS, 2 Kapitanskaya Street, Sevastopol, Russia 299011

<sup>2</sup> The A.O. Kovalevsky Institute of Marine Biological Research of RAS, 2 Nakhimov Prospect, Sevastopol, Russia 299011

$\text{NH}_4\text{MgPO}_4 \cdot 6\text{H}_2\text{O}$ , separation of impurities by on cation and anion exchange, preparation of a counting sample for  $\beta$ -radiometry in the form of  $\text{NH}_4\text{MgPO}_4 \cdot 6\text{H}_2\text{O}$  were described. In the works of Benitez-Nelson et al. [9, 13, 22] similar procedures were used, but the concentration of the  $^{32}\text{P}$  and  $^{33}\text{P}$  was performed by coprecipitation with  $\text{Fe}(\text{OH})_3$ , and the liquid-scintillation spectrometry using a liquid sample obtained after purification on ion exchange resins was used for the measurement. The same technique was also applied in [23, 24] and used as the basic procedure in this work.

$^7\text{Be}$  is also a radionuclide ( $T_{1/2} = 53.3$  days,  $E_\gamma = 0.477$  MeV) of cosmogenic origin [25]. It is continuously produced in the atmosphere (2/3 in the stratosphere and 1/3 in the troposphere) by spallation processes of light atmospheric nuclei such as carbon  $^{12}\text{C}$ , nitrogen  $^{14}\text{N}$ , and oxygen  $^{16}\text{O}$ , with primary and secondary components of cosmic rays (protons and neutrons, respectively) [26]. From the atmosphere to the earth's surface it transported mostly by wet precipitation [27]. This radionuclide is convenient to trace various processes governing its distribution and re-distribution in the environment on the short time scales: investigation of air mass dynamics [28], studies surface water subduction and mixed-layer history [29], estimation of flux of other isotopes and chemical compounds with precipitation [30, 31], etc.

In order to numerically model a migration of  $^7\text{Be}$  in the environment (marine or atmospheric), the information on boundary conditions (deposition of  $^7\text{Be}$  from the atmosphere at the surface) was of primary interest. Data on the spatial and temporal variability of  $^7\text{Be}$  atmospheric flux were also important and necessary for investigating specific features of the radionuclide wet deposition mechanism.

To date the  $^7\text{Be}$  flux measurements were performed in different regions of the Earth, but to the best of our knowledge, those data were not available for the Black Sea region [32]. At the present time, we are studying  $^7\text{Be}$  in the Black Sea and plan to study  $^{32}\text{P}$  and  $^{33}\text{P}$ . We need to know the atmospheric fluxes of these radionuclides for modeling processes in the sea.

In a number of studies the dominant factors accounting for the temporal variability in the  $^7\text{Be}$  flux were highlighted [33, 34]. According to the latter, wet deposition of  $^7\text{Be}$  depended on the type, amount, and frequency of precipitation as well as the isotope content in the atmosphere. The surface activity concentration of  $^7\text{Be}$  in the ambient air is controlled by four processes [35]: (i) stratosphere–troposphere exchange associated with tropopause folding near the polar front and subtropical jet stream [36, 37], or with large cut-off lows [38, 39]; (ii) vertical downward transport in the troposphere which can be attributed to more efficient vertical mixing in the warm season due to enhanced solar

heating; (iii) wet scavenging of atmospheric aerosols [40]; (iv) advection from the mid-latitudes to higher and lower latitudes [41]. Besides this, surface  $^7\text{Be}$  concentrations vary depending on solar activity, season, location and local meteorological conditions [42, 43].

The analysis of current temporal variability studies in  $^{32}\text{P}$ ,  $^{33}\text{P}$  and  $^7\text{Be}$  wet depositions were presented for the region where those data were not available before. The primary objective of this study was to investigate the relationship between the flux values and the precipitation amounts for the radionuclides in question as well as to estimate the annual wet deposition of these radionuclides in Sevastopol region for the period of 11 months.

## Experimental

### Materials

Nitric acid, hydrochloric acid, ammonia, iron(3+) chloride, magnesium chloride, ammonium chloride (ReaKhim, Russia) were of analytical reagent grade and were used as received. Cation KU-2-8 and anion AV-17-8 exchange resins and Dowex HCR-S/S cation exchange resin were commercially available samples manufactured by the “Resins” State Enterprise (Dneprodzerzhinsk, Ukraine) and Dow Chemical Co. (USA), respectively. The nitrocellulose « Vladisart » membrane (0.45  $\mu\text{m}$  pore-size, 47 mm in diameter) was obtained from CJSC “Vladisart”, Vladimir City, Russia.

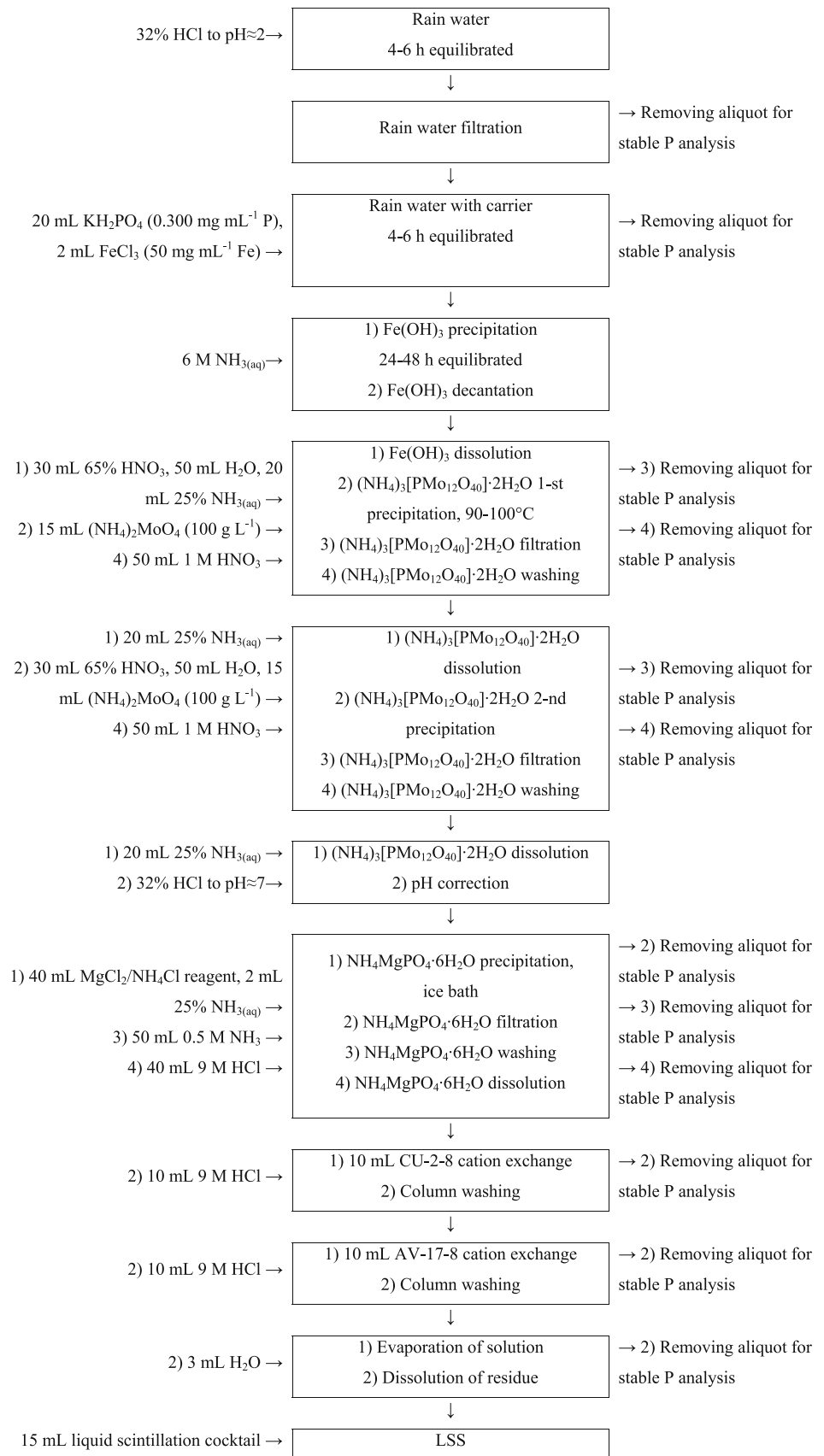
### Collection of atmospheric wet depositions

Individual rainwater samples were collected on the roof of the Marine Hydrophysical Institute (44°36'55.9''N, 33°31'01.6''E) in enameled cuvette shaped cells of 0.64 m<sup>2</sup> square area located at a height of 1.5 m above the underlying roofing surface level. The cells were connected with a 50 L plastic container to minimize evaporation losses. The collected rainwater samples were conditioned by acidifying with concentrated HCl to obtain a pH of  $\sim 2$  (10 mL acid per 1.0 L of sample), keeping samples for 4–6 h, and filtering.

During the whole 2016 year for all rainfall events of more than 1.0 mm day<sup>-1</sup> wet deposition samples were collected to determine the specific activity of  $^7\text{Be}$ . Once a month individual samples were collected to determine the specific activities of  $^{32}\text{P}$  and  $^{33}\text{P}$ .

### Separation and purification of phosphorus

The radiochemical preparation (Fig. 1) was performed as described in [23, 24]; the precipitation techniques used

**Fig. 1** Flow chart for chemical purification

were as described in classical analytical chemistry [44]. The sample and precipitate filtering and washing was performed on single use disposable “Vladisart” membranes.

The solutions containing 100 mg of  $\text{Fe}^{3+}$  (2 mL of  $\text{FeCl}_3$  solution with an  $\text{Fe}^{3+}$  concentration of  $50 \text{ mg mL}^{-1}$ ) and 6 mg of a non-radioactive P carrier (20 mL of a  $\text{KH}_2\text{PO}_4$  solution with a concentration of  $0.3 \text{ mg mL}^{-1}$ ) were added to the conditioned rainwater samples followed by equilibrating the mix for 4–6 h.

Phosphorus was coprecipitated with  $\text{Fe}(\text{OH})_3$  using 6 M ammonia solution by adding it slowly stirring to reach a slightly alkaline medium. The mix was allowed to settle during 24–48 h for precipitate ageing and then decanted to final suspension volume about 100 mL.

For precipitating  $(\text{NH}_4)_3[\text{PMo}_{12}\text{O}_{40}] \cdot 2\text{H}_2\text{O}$  the suspension of  $\text{Fe}(\text{OH})_3$  was dissolved in 30 mL of concentrated  $\text{HNO}_3$ , and then 50 mL of  $\text{H}_2\text{O}$  and 20 mL of 25%  $\text{NH}_3(\text{aq})$  were added. The sample was heated to the boiling point and then 15 mL of ammonium molybdate ( $100 \text{ g L}^{-1}$ ) solution was added dropwise under continuous stirring. The obtained  $(\text{NH}_4)_3[\text{PMo}_{12}\text{O}_{40}] \cdot 2\text{H}_2\text{O}$  was filtered after 20 min and washed with 50 mL of 1 M  $\text{HNO}_3$  on the filter. The precipitate was dissolved from the filter in 20 mL of 25%  $\text{NH}_3(\text{aq})$  and 50 mL of  $\text{H}_2\text{O}$ . Then 30 mL of 65%  $\text{HNO}_3$  was added and a second precipitation of  $(\text{NH}_4)_3[\text{PMo}_{12}\text{O}_{40}] \cdot 2\text{H}_2\text{O}$  was performed by adding 15 mL solution of ammonium molybdate ( $100 \text{ g L}^{-1}$ ).

Prior to the preparation of  $\text{NH}_4\text{MgPO}_4 \cdot 6\text{H}_2\text{O}$  the  $\text{MgCl}_2/\text{NH}_4\text{Cl}$  reagent was freshly made by mixing 55 g of  $\text{MgCl}_2 \cdot 6\text{H}_2\text{O}$ , 105 g of  $\text{NH}_4\text{Cl}$ , 350 mL of the 25%  $\text{NH}_3(\text{aq})$ , till the volume of the mix up to 1 L by  $\text{H}_2\text{O}$  and filtering the solution obtained.

The purified  $(\text{NH}_4)_3[\text{PMo}_{12}\text{O}_{40}] \cdot 2\text{H}_2\text{O}$  precipitate was dissolved from the filter in 20 mL of 25%  $\text{NH}_3(\text{aq})$ , and the pH was adjusted to 7 with the 32%  $\text{HCl}$  (about 17 mL). Then 40 mL of the above mentioned  $\text{MgCl}_2/\text{NH}_4\text{Cl}$  reagent and 2 mL of the concentrated  $\text{NH}_3$  in an ice bath were added to the solution. The  $\text{NH}_4\text{MgPO}_4 \cdot 6\text{H}_2\text{O}$  precipitate was filtered and washed with 50 mL of 0.5 M  $\text{NH}_3(\text{aq})$ .

The  $\text{NH}_4\text{MgPO}_4 \cdot 6\text{H}_2\text{O}$  precipitate was dissolved in 40 mL of 9 M  $\text{HCl}$  and the resulting solution was passed through a column contains 10 mL of KU-2-8 cation exchange resin in  $\text{H}^+$ -form. Then the cation resin column was purged with 10 mL of 9 M  $\text{HCl}$ , and the emerging eluate was passed through another resin containing 10 mL of AV-17-8 anion exchange resin in  $\text{Cl}^-$ -form. Then, the anion resin was purged with 10 mL of 9 M  $\text{HCl}$ , the emerging eluate was collected, evaporated to dryness, and the dry residue was dissolved in 3 mL of  $\text{H}_2\text{O}$ . Finally, 15 mL of the liquid scintillation cocktail OptiPhase HiSafe III was added to the latter to prepare the sample for liquid scintillation counting.

For the determination of the phosphorus yield along the sample preparation steps the classical molybdenum blue method [45] was used. Solutions examined were as follows: the initial feed, solution after adding the natural phosphorus, solutions before (200  $\mu\text{L}$  samples) and after the first  $(\text{NH}_4)_3[\text{PMo}_{12}\text{O}_{40}] \cdot 2\text{H}_2\text{O}$  precipitation stage, solution after the second  $(\text{NH}_4)_3[\text{PMo}_{12}\text{O}_{40}] \cdot 2\text{H}_2\text{O}$  precipitation stage, solutions after the first and the second washing of  $(\text{NH}_4)_3[\text{PMo}_{12}\text{O}_{40}] \cdot 2\text{H}_2\text{O}$ , solutions after the precipitation of ammonium phosphate  $\text{NH}_4\text{MgPO}_4 \cdot 6\text{H}_2\text{O}$ , solutions after washing of  $\text{NH}_4\text{MgPO}_4 \cdot 6\text{H}_2\text{O}$ , solutions after cation and anion exchange columns (200  $\mu\text{L}$  samples of each), and in the final solution (100  $\mu\text{L}$  sample). We had volumes larger than necessary for analysis in most cases, an aliquot of 10 mL was usually taken.

### $^{32}\text{P}$ and $^{33}\text{P}$ measurements

$^{32}\text{P}$  and  $^{33}\text{P}$  were measured by the Wallac 1220 Quantulus (Perkin Elmer Co) ultra-low-level liquid scintillation spectrometer (LSS). For  $^{32}\text{P}$  and  $^{33}\text{P}$  ( $E_{\text{max}} > 156 \text{ keV}$ ), the counting efficiency was usually higher than 95% [23]. The uncertainty did not usually exceed 10%.

### Separation and purification of $^7\text{Be}$

Pre-concentration of  $^7\text{Be}$  from rainwater samples was conducted using two columns loaded with the Dowex HCR-S/S cation exchange resin connected in series [46]. The sorption efficiency was determined from the distribution of  $^7\text{Be}$  activity between the above two columns according to the following equation [24]:

$$\text{Collection efficiency} = 1 - B/A, \quad (1)$$

where  $A$  and  $B$  were the  $^7\text{Be}$  activity of the first and the second column in series, respectively.

### $^7\text{Be}$ measurements

Measurements of the  $^7\text{Be}$  activity in the samples were carried out using a low-background gamma-spectrometer equipped with a  $\text{NaI}(\text{TI})$  scintillation detector (diameter—63 mm, height—63 mm, the resolution of 7.5% from the peak of  $^{137}\text{Cs}$ ). The detector was located on the ground floor of a three-storey building and shielded by cast iron and lead rings of 150 and 140 mm width, respectively. Registration and processing of the spectrometric data were performed by the software installed on an IBM PC. Each sample was measured for 12–15 h, and the data were automatically recorded every 3 h to the memory of the PC. To determine the 477.7 keV efficiency ( $^7\text{Be}$   $\gamma$ -ray), some

samples were measured on both the above-mentioned gamma spectrometer and a gamma spectrometer with a coaxial HPGe detector. The energy calibration of the gamma spectrometer with the coaxial HPGe detector was performed using certified mixed sources. The uncertainty was determined by the statistical error of the sample activity measurement ( $2\sigma$ ) and usually did not exceed 12%.

### Results and discussion

Phosphorus losses along the sample preparation steps are presented in Table 1. The primary steps for phosphorus losses occur as follows: decanting, precipitation of  $(\text{NH}_4)_3[\text{PMo}_{12}\text{O}_{40}]\cdot 2\text{H}_2\text{O}$ , cation and anion.

According to Lal, the total yield of phosphorus by radiochemical analysis was 50–80% [2]; according to Benitez-Nelson and Buessler the value in question ranged within 31.6–90.8%, averaging 68.6% [11]. Chen [23] reported the yield of phosphorus by steps as follows:  $\text{Fe}(\text{OH})_3$  co-precipitation—89–91%;  $(\text{NH}_4)_3\text{PO}_4(\text{MoO}_3)_2$  precipitation—92.4–94.2%;  $\text{NH}_4\text{MgPO}_4\cdot 6\text{H}_2\text{O}$  precipitation—93–99%. Losses during the precipitation of ammonium phosphomolybdate could be reduced keeping the precipitate up to the next day, but it greatly increased the sample preparation time, which adversely affected the analysis of short-lived  $^{32}\text{P}$  and  $^{33}\text{P}$  radionuclides. In this work the average phosphorus yield value was  $53.4 \pm 18.5\%$ .

Low yields for  $^7\text{Be}$  (Table 2) were associated with high elution rates through the columns. Nevertheless, this fact did not produce a great error, since the sufficient activity (not less than 1 Bq) required to determine the reliable yield value was retained on the second column. In the case of beryllium, small values of the yield (R2 and R3 samples) were also observed when large sample volumes were filtered through the columns. It could be associated with the

**Table 1** Losses of phosphorus by the radiochemical preparation stages (at least 3 experiments for each stage, 6 experiments for precipitation and washing of  $(\text{NH}_4)_3[\text{PMo}_{12}\text{O}_{40}]\cdot 2\text{H}_2\text{O}$ )

Preparation stage	Phosphorus loss $\pm \sigma$ (%)
Coprecipitation, decanting	12.55 $\pm$ 4.88
Precipitation of $(\text{NH}_4)_3[\text{PMo}_{12}\text{O}_{40}]\cdot 2\text{H}_2\text{O}$	5.44 $\pm$ 2.01
Washing of $(\text{NH}_4)_3[\text{PMo}_{12}\text{O}_{40}]\cdot 2\text{H}_2\text{O}$	0.05 $\pm$ 0.02
Precipitation of $\text{NH}_4\text{MgPO}_4\cdot 6\text{H}_2\text{O}$	0.43 $\pm$ 0.34
Washing of $\text{NH}_4\text{MgPO}_4\cdot 6\text{H}_2\text{O}$	0.35 $\pm$ 0.19
Anion exchange	5.46 $\pm$ 2.24
Cation exchange	7.00 $\pm$ 4.75

**Table 2**  $^{32}\text{P}$ ,  $^{33}\text{P}$ , and  $^7\text{Be}$  in rainwater samples

Sample no.	Date (year-month-day)	Rainfall (mm)	Maximum wind speed (m s <sup>-1</sup> )	Yield of P (%)	Yield of $^7\text{Be}$ (%)	Specific activity of $^{33}\text{P}$ (dpm L <sup>-1</sup> )	Specific activity of $^{32}\text{P}$ (dpm L <sup>-1</sup> )	Specific activity of $^7\text{Be}$ (dpm L <sup>-1</sup> )	Flux of $^{33}\text{P}$ (dpm m <sup>-2</sup> day <sup>-1</sup> )	Flux of $^{32}\text{P}$ (dpm m <sup>-2</sup> day <sup>-1</sup> )	Flux of $^7\text{Be}$ (dpm m <sup>-2</sup> day <sup>-1</sup> )	$^{33}\text{P}/^{32}\text{P}$ ratio	$^7\text{Be}/^{33}\text{P}$ ratio	$^7\text{Be}/^{32}\text{P}$ ratio
R1	16-02-26	2.0	11.2	66.5	53.6	1.47 $\pm$ 0.11	1.92 $\pm$ 0.12	432.0 $\pm$ 86.4	2.94 $\pm$ 0.22	3.84 $\pm$ 0.23	843.8 $\pm$ 168.8	0.77 $\pm$ 0.23	287 $\pm$ 87	220 $\pm$ 87
R2	16-03-23	10.6	17.0	57.2	25.5	1.49 $\pm$ 0.10	1.56 $\pm$ 0.09	138.4 $\pm$ 37.4	15.82 $\pm$ 1.09	16.54 $\pm$ 0.99	1470.6 $\pm$ 397.1	0.96 $\pm$ 0.20	93 $\pm$ 38	89 $\pm$ 37
R3	16-04-27	15.6	15.2	53.0	19.7	2.43 $\pm$ 0.07	2.42 $\pm$ 0.07	256.9 $\pm$ 28.3	37.84 $\pm$ 1.02	37.77 $\pm$ 1.09	4013.5 $\pm$ 441.5	1.00 $\pm$ 0.14	106 $\pm$ 28	106 $\pm$ 28
R4	16-05-25	2.7	10.7	17.1	46.4	2.51 $\pm$ 0.13	3.09 $\pm$ 0.14	413.5 $\pm$ 33.1	6.79 $\pm$ 0.35	8.33 $\pm$ 0.39	1130.8 $\pm$ 90.5	0.81 $\pm$ 0.27	167 $\pm$ 33	136 $\pm$ 33
R5	16-06-13	2.5	16.1	40.8	50.5	3.48 $\pm$ 0.19	2.67 $\pm$ 0.15	135.9 $\pm$ 21.7	8.71 $\pm$ 0.48	6.68 $\pm$ 0.37	339.8 $\pm$ 54.4	1.30 $\pm$ 0.34	39 $\pm$ 22	51 $\pm$ 22
R6	16-07-10	6.6	21.9	58.7	62.7	1.53 $\pm$ 0.08	1.26 $\pm$ 0.06	174.3 $\pm$ 13.1	10.11 $\pm$ 0.53	8.34 $\pm$ 0.41	1143.8 $\pm$ 85.8	1.21 $\pm$ 0.14	113 $\pm$ 13	137 $\pm$ 13
R7	16-08-06	5.0	25.9	82.9	58.3	1.83 $\pm$ 0.09	1.31 $\pm$ 0.07	312.5 $\pm$ 18.8	9.14 $\pm$ 0.44	6.56 $\pm$ 0.34	1562.5 $\pm$ 93.8	1.39 $\pm$ 0.16	171 $\pm$ 19	238 $\pm$ 19
R8	16-09-29	2.0	13.0	69.7	64.7	2.07 $\pm$ 0.12	2.76 $\pm$ 0.14	189.9 $\pm$ 32.3	4.15 $\pm$ 0.24	5.52 $\pm$ 0.29	385.7 $\pm$ 65.6	0.75 $\pm$ 0.27	93 $\pm$ 32	70 $\pm$ 32
R9	16-10-08	8.4	16.5	30.1	38.4	3.63 $\pm$ 0.16	2.82 $\pm$ 0.14	146.5 $\pm$ 8.8	30.48 $\pm$ 1.38	23.68 $\pm$ 1.16	1235.9 $\pm$ 74.2	1.29 $\pm$ 0.30	41 $\pm$ 9	52 $\pm$ 9
R10	16-11-10	3.0	21.0	60.1	35.4	5.18 $\pm$ 0.19	3.81 $\pm$ 0.15	533.7 $\pm$ 48.0	15.55 $\pm$ 0.56	11.44 $\pm$ 0.46	1584.4 $\pm$ 142.6	1.36 $\pm$ 0.34	102 $\pm$ 48	138 $\pm$ 48
R11	16-12-11	5.5	17.9	51.1	46.0	2.16 $\pm$ 0.11	1.62 $\pm$ 0.09	297.8 $\pm$ 23.8	11.89 $\pm$ 0.61	8.93 $\pm$ 0.48	1638.0 $\pm$ 131.0	1.33 $\pm$ 0.20	138 $\pm$ 24	183 $\pm$ 24
Mean $\pm \sigma$		5.8 $\pm$ 4.3	17.0 $\pm$ 4.6	53.4 $\pm$ 18.5	46.0 $\pm$ 14.7	2.53 $\pm$ 1.15	2.29 $\pm$ 0.82	276.0 $\pm$ 136.0	13.95 $\pm$ 10.90	12.51 $\pm$ 10.10	1395.0 $\pm$ 979.0	1.11 $\pm$ 0.25	123 $\pm$ 69	129 $\pm$ 64

resin capacity exhausted by the accompanying cations present in the sample.

### Temporal variability of isotope fallout with wet atmospheric deposition

During the period of time starting from January through December 2016, 45 samples of rain water were collected to determine the  $^7\text{Be}$  specific activity (Fig. 2).

Eleven samples out of the collected 45 were selected for the additional determination of the specific activity of  $^{33}\text{P}$  and  $^{32}\text{P}$  radionuclides (Table 2; Figs. 3, 4, 5, 6). The reported specific activities were corrected to decay to the

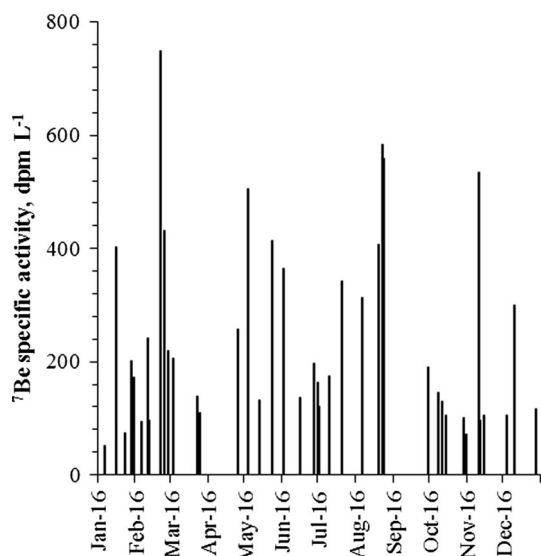


**Fig. 2** Temporal variability of the  $^7\text{Be}$  specific activity in atmospheric precipitations

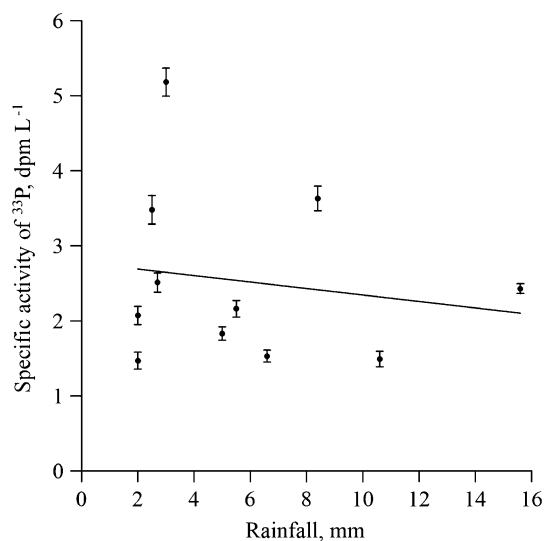


**Fig. 3** The specific activity of  $^{33}\text{P}$  versus rainfall amount

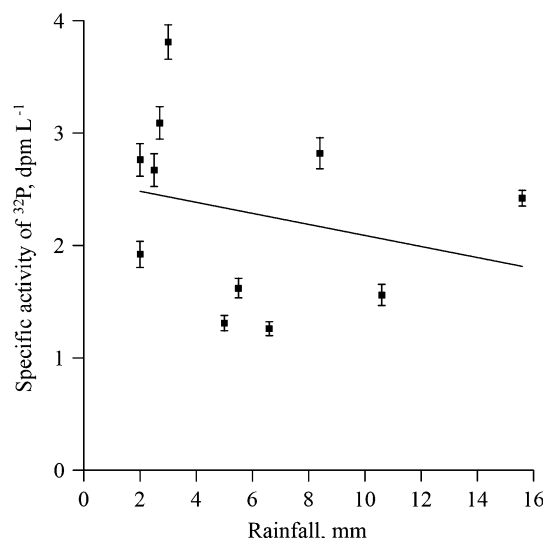


**Fig. 4** The specific activity of  $^{32}\text{P}$  versus rainfall amount

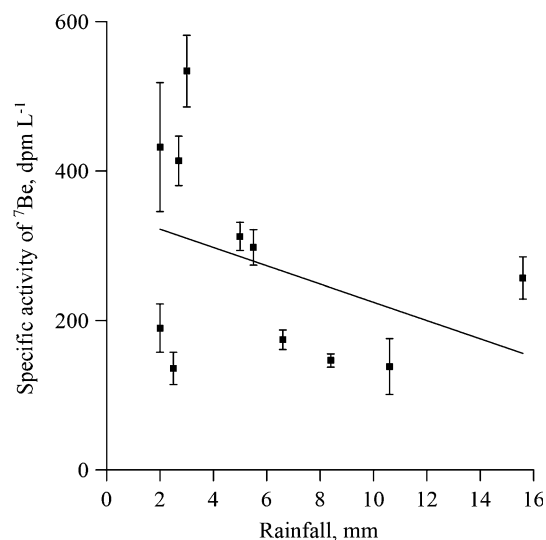


**Fig. 5** The specific activity of  $^7\text{Be}$  versus rainfall amount

time of sample collection. The isotope flux values and their ratios were calculated from the specific activities. The results obtained showed that the specific activity of  $^{33}\text{P}$  varied within the range of  $1.47\text{--}5.18\text{ dpm L}^{-1}$ , the average value being  $2.53\text{ dpm L}^{-1}$ ; the specific activity of  $^{32}\text{P}$  was in the range of  $1.26\text{--}3.81\text{ dpm L}^{-1}$ , the average value being  $2.29\text{ dpm L}^{-1}$ , and for  $^7\text{Be}$  the range was  $51.7\text{--}749.1\text{ dpm L}^{-1}$  ( $0.86\text{--}12.5\text{ Bq L}^{-1}$ ), the average value being  $240.5\text{ dpm L}^{-1}$  ( $4\text{ Bq L}^{-1}$ ). The reference data from the studies conducted at close latitudes showed similar values as follows: from  $0.27\text{ to }13.61\text{ dpm L}^{-1}$  for  $^{33}\text{P}$  and  $^{32}\text{P}$  and from  $21\text{ to }1442\text{ dpm L}^{-1}$  for  $^7\text{Be}$  [9]. As the amount of atmospheric precipitations increased, the specific activity of the isotopes decreased. This phenomenon indicated that the rainfall rate played an

**Fig. 6** The daily flux of  $^{33}\text{P}$ ,  $^{32}\text{P}$  and  $^7\text{Be}$

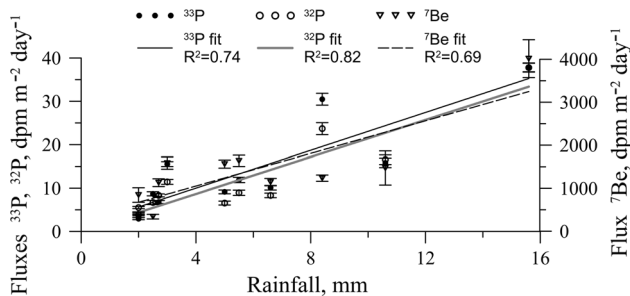
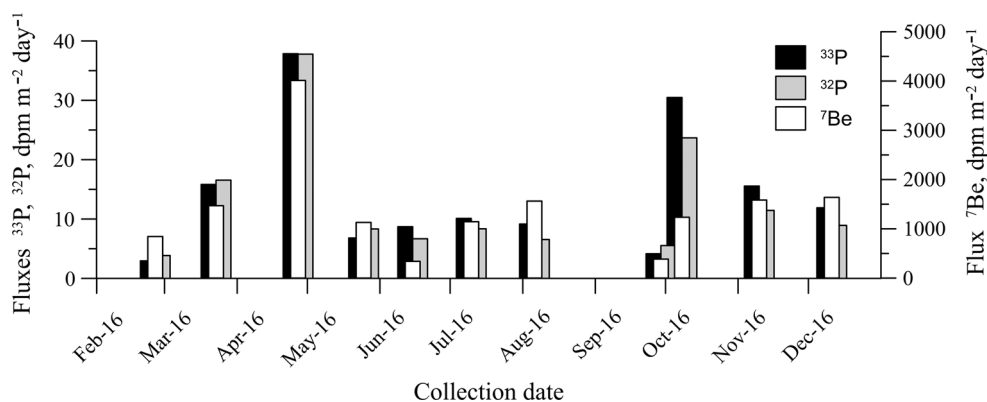


**Fig. 7** The daily flux of  $^{33}\text{P}$ ,  $^{32}\text{P}$  and  $^7\text{Be}$  versus rainfall amount

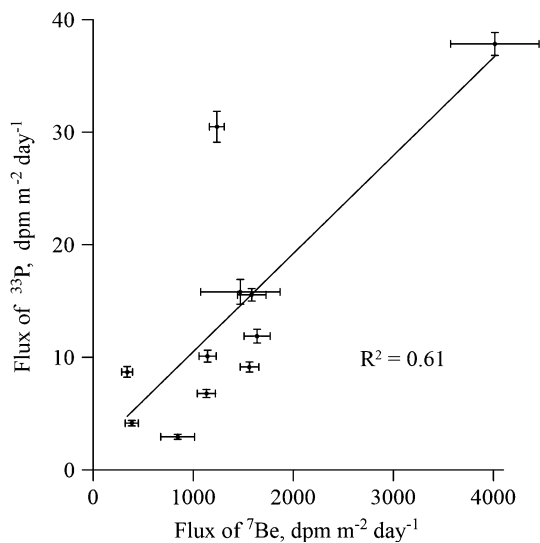


**Fig. 8** The daily flux of  $^{33}\text{P}$  versus daily flux of  $^7\text{Be}$

important role in the removal of these isotopes from the troposphere, which is concordance with [9, 40].

The calculated flux values are given in Table 2. The flux varied from 2.94 to 37.84  $\text{dpm m}^{-2} \text{day}^{-1}$  for  $^{33}\text{P}$ , the average value being 13.95  $\text{dpm m}^{-2} \text{day}^{-1}$ ; for  $^{32}\text{P}$  it was within 3.84 through 37.77  $\text{dpm m}^{-2} \text{day}^{-1}$ , the average value being 12.51  $\text{dpm m}^{-2} \text{day}^{-1}$ ; and for  $^7\text{Be}$  it was 176.6–4345.8  $\text{dpm m}^{-2} \text{day}^{-1}$  (2.9–72.4  $\text{Bq m}^{-2} \text{day}^{-1}$ ,

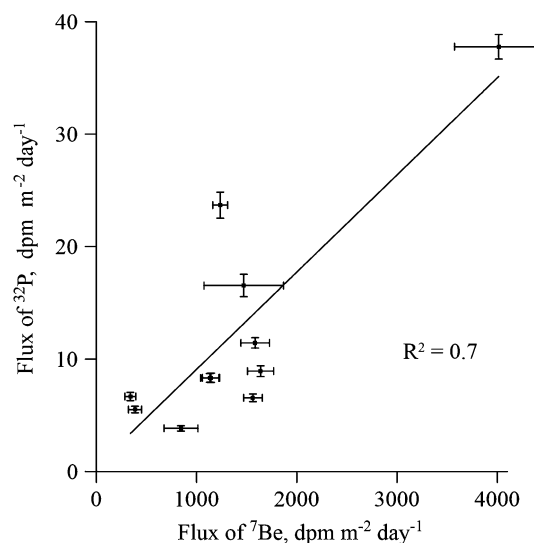


**Fig. 9** The daily flux of  $^{32}\text{P}$  versus daily flux of  $^7\text{Be}$

the whole data array was used), the average value being 1177  $\text{dpm m}^{-2} \text{day}^{-1}$  (19.6  $\text{Bq m}^{-2} \text{day}^{-1}$ ).

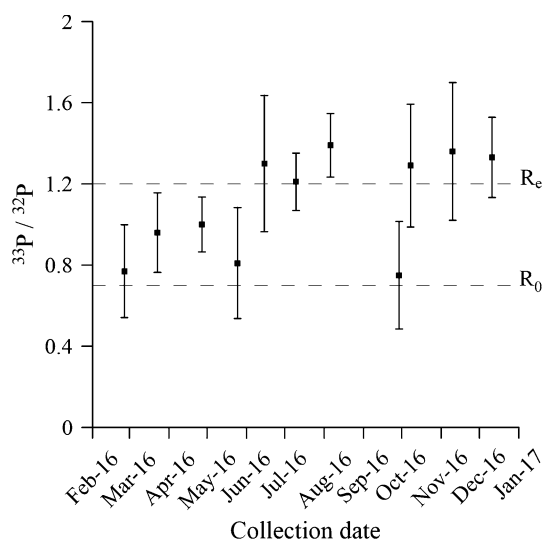
The dependence of the flux values on the rainfall amount is shown in Fig. 7. An increase in the rainfall amount led to an increase in isotope fluxes. Deviations in the flux-rainfall relationships among the radionuclides could arise from the difference in air mass sources, scavenging rates, and radioactive decay. There is a reasonably significant correlation of 0.79 between the fluxes of  $^{33}\text{P}$  and  $^7\text{Be}$  and of 0.85 between the fluxes of  $^{32}\text{P}$  and  $^7\text{Be}$  (Figs. 8, 9).

Using the row daily  $^7\text{Be}$  wet deposition data and the flux value relationship (Figs. 8, 9) the estimates of total monthly and annual flux of  $^{33}\text{P}$  and  $^{32}\text{P}$  with precipitations were made (Table 3). The maximum flux values were observed in the winter period, the minimum values were observed in autumn.

The total annual flux values  $^{33}\text{P}$  and  $^{32}\text{P}$  (Table 3) obtained in Woods Hole (41.32°N) [9]—0.165  $\text{dpm cm}^{-2} \text{year}^{-1}$  (1650  $\text{dpm m}^{-2} \text{year}^{-1}$ ) for  $^{33}\text{P}$ ; 0.178  $\text{dpm cm}^{-2} \text{year}^{-1}$

**Table 3** The monthly and annual flux of  $^{32}\text{P}$ ,  $^{33}\text{P}$ , and  $^7\text{Be}$ 

Month	Rainfall (mm)	Flux of $^7\text{Be}$ (dpm $\text{m}^{-2}$ )	Flux of $^{32}\text{P}$ (dpm $\text{m}^{-2}$ )	Flux of $^{33}\text{P}$ (dpm $\text{m}^{-2}$ )
Jan-2016	43.0	7643	68	75
Feb-2016	32.8	5193	47	56
Mar-2016	17.8	2621	24	28
Apr-2016	15.6	4013	35	37
May-2016	12.2	3983	36	40
Jun-2016	19.8	3854	35	41
Jul-2016	18.9	2878	26	30
Aug-2016	14.2	6403	57	63
Sep-2016	2.0	386	4	5
Oct-2016	58.8	6249	56	63
Nov-2016	17.8	3263	30	36
Dec-2016	26.4	6485	59	67
Annual	279.4	52,971	476	542

**Fig. 10** The  $^{33}\text{P}/^{32}\text{P}$  activity ratio in rainwater samples

(1780 dpm  $\text{m}^{-2}$  year $^{-1}$ ) for  $^{32}\text{P}$ ; in Bermuda (32.3°N) [20]—0.082 dpm  $\text{cm}^{-2}$  year $^{-1}$  (820 dpm  $\text{m}^{-2}$  year $^{-1}$ ) for  $^{33}\text{P}$ ; 0.086 dpm  $\text{cm}^{-2}$  year $^{-1}$  (860 dpm  $\text{m}^{-2}$  year $^{-1}$ ) for  $^{32}\text{P}$ ; in Bombay (19°N) [47]—0.15 dpm  $\text{cm}^{-2}$  year $^{-1}$  (1500 dpm  $\text{m}^{-2}$  year $^{-1}$ ) for  $^{33}\text{P}$ ; 0.087 dpm  $\text{cm}^{-2}$  year $^{-1}$  (870 dpm  $\text{m}^{-2}$  year $^{-1}$ ) for  $^{32}\text{P}$ ; global estimates [4]—0.069 dpm  $\text{cm}^{-2}$  year $^{-1}$  (690 dpm  $\text{m}^{-2}$  year $^{-1}$ ) for  $^{33}\text{P}$ ; 0.104 dpm  $\text{cm}^{-2}$  year $^{-1}$  (1040 dpm  $\text{m}^{-2}$  year $^{-1}$ ) for  $^{32}\text{P}$ .

The  $^7\text{Be}$  flux values obtained in Woods Hole (41.32°N) [9]—12.8 dpm  $\text{cm}^{-2}$  year $^{-1}$  (128,000 dpm  $\text{m}^{-2}$  year $^{-1}$ ); in Monaco (43.8°N) [48] were vary from 390 to 2000 Bq  $\text{m}^{-2}$  year $^{-1}$  (from 23,400 to 120,000 dpm  $\text{m}^{-2}$  year $^{-1}$ ), in Huelva, Spain (37.3°N) [49] it was 834 Bq  $\text{m}^{-2}$  year $^{-1}$  (50,040 dpm  $\text{m}^{-2}$  year $^{-1}$ ), in Thessaloniki, Greece (40.6°N) [50] they were vary from 483 to 841 Bq  $\text{m}^{-2}$  year $^{-1}$  (from 28,980 to 50,460 dpm  $\text{m}^{-2}$  year $^{-1}$ ).

Maximum flux values coincide with the peaks of precipitation amounts [9, 20, 48, 49]. Maximum flux values in Monaco were observed in fall and the minimum—in summer [48], in Huelva, Spain and Thessaloniki, Greece they were in winter and summer seasons, respectively [49, 50].

The difference in the flux values  $^{33}\text{P}$ ,  $^{32}\text{P}$  and  $^7\text{Be}$  (Table 3) may be due to the difference in precipitation rate 27.9 cm year $^{-1}$  in the Sevastopol region, compared to 84.8 cm year $^{-1}$  in Woods Hole [9], 47 cm per year in Bermuda [20], 22.3–100.6 cm year $^{-1}$  in Monaco [48], 85.9 cm year $^{-1}$  in Huelva, Spain [49], 32.6–65.0 cm year $^{-1}$  in Thessaloniki, Greece [50].

The flux ratio values of  $^{33}\text{P}/^{32}\text{P}$  and  $^7\text{Be}/^{33}\text{P}$  were calculated (Table 2; Fig. 10). The minimum value was 0.75 and 51, the maximum value was 1.39 and 238, the average being 1.1 and 129 for  $^{33}\text{P}/^{32}\text{P}$  and  $^7\text{Be}/^{33}\text{P}$ , respectively.

In [51] the initial production ratio ( $R_0$ ) and the equilibrium ratio ( $R_e$ ) values for  $^{33}\text{P}$  and  $^{32}\text{P}$  were estimated. According to the results obtained,  $R_0$  varied in the range of 0.46–0.7, and the maximum possible value for  $R_e$  was 1.2. In [52] the  $^{33}\text{P}/^{32}\text{P}$  ratio value in the stratospheric air masses of 0.9 was reported, therefore, a value of  $^{33}\text{P}/^{32}\text{P}$  greater than 0.9 indicated a stratospheric source of air masses. In [9] it was also reported that the higher  $^{33}\text{P}/^{32}\text{P}$  values were observed under storm conditions. According to our data, lower  $^{33}\text{P}/^{32}\text{P}$  ratios (samples R1, R4, and R8) were observed at maximum wind speeds of less than 6 grades on the Beaufort scale (Breeze winds). Higher  $^{33}\text{P}/^{32}\text{P}$  ratios (the remaining samples) were observed, as a rule, at wind speeds of more than 8 grades on the Beaufort scale (Gale, Strong, and Storm winds). We also note the presence of a strong statistically significant correlation between the  $^{33}\text{P}/^{32}\text{P}$  and the maximum wind speed, the correlation coefficient being 0.8. The  $^7\text{Be}/^{33}\text{P}$  ratio could



not be used for investigation of the stratosphere to troposphere exchange [9].

## Conclusions

Specific activity values of  $^{32}\text{P}$ ,  $^{33}\text{P}$ , and  $^7\text{Be}$  were determined in rainwater samples collected during the year 2016 in the Sevastopol region. The  $^{32}\text{P}$ ,  $^{33}\text{P}$ , and  $^7\text{Be}$  flux values were calculated. The results obtained showed that the mean flux values with precipitations were  $13.95 \text{ dpm m}^{-2} \text{ day}^{-1}$  for  $^{33}\text{P}$ ,  $12.51 \text{ dpm m}^{-2} \text{ day}^{-1}$  for  $^{32}\text{P}$ , and  $1177 \text{ dpm m}^{-2} \text{ day}^{-1}$  for  $^7\text{Be}$ .

Using flux relationships of  $^{32}\text{P}$  vs.  $^7\text{Be}$  and  $^{33}\text{P}$  vs.  $^7\text{Be}$  monthly and annual flux values of  $^{32}\text{P}$  and  $^{33}\text{P}$  with atmospheric precipitations were calculated. The maximum monthly flux values for the isotopes under study were observed in the winter period, the minimum values were observed in autumn. The annual flux values with precipitations were  $542 \text{ dpm m}^{-2} \text{ year}^{-1}$  for  $^{33}\text{P}$ ,  $476 \text{ dpm m}^{-2} \text{ year}^{-1}$  for  $^{32}\text{P}$ , and  $52,971 \text{ dpm m}^{-2} \text{ year}^{-1}$  for  $^7\text{Be}$  ( $\sim 883 \text{ Bq m}^{-2} \text{ year}^{-1}$ ).

**Acknowledgements** The research was performed under the state assignment of FASO of the Russian Federation (the “Fundamental oceanography” research topic No. 0827-2014-0010), supported in part by Russian Foundation for Basic Research (RFBR) (Project No. 16-05-00206). We thank anonymous referee and the journal editor whose constructive comments proved very useful in improving an earlier version of the paper.

## References

1. Marquez L, Costa NL (1955) The formation of  $^{32}\text{P}$  from atmospheric argon by cosmic rays. *Nuovo Cimento* 2(5):1038–1041. <https://doi.org/10.1007/BF02855849>
2. Lal D, Narasappaya N, Zutshi PK (1957) Phosphorus isotopes  $\text{P}^{32}$  and  $\text{P}^{33}$  in rain water. *Nucl Phys* 3(1):69–75. [https://doi.org/10.1016/0029-5582\(57\)90054-8](https://doi.org/10.1016/0029-5582(57)90054-8)
3. Lal D (1999) An overview of five decades of studies of cosmic ray produced nuclides in oceans. *Sci Total Environ* 237–238:3–13. [https://doi.org/10.1016/S0048-9697\(99\)00120-5](https://doi.org/10.1016/S0048-9697(99)00120-5)
4. Lal D, Peters B (1967) Cosmic ray produced radioactivity on the earth. In: Sitte K (ed) *Kosmische strahlung II/cosmic rays II*. *Handbuch der physik/encyclopedia of physics*, vol 9/46/2. Springer, Berlin
5. Benitez-Nelson CR (2000) The biogeochemical cycling of phosphorus in marine systems. *Earth-Sci Rev* 51(1–4):109–135. [https://doi.org/10.1016/S0012-8252\(00\)00018-0](https://doi.org/10.1016/S0012-8252(00)00018-0)
6. Ruttenger KC (2014) The global phosphorus cycle. In: Holland HD, Turekian KK (eds) *Treatise on geochemistry*. Elsevier, Oxford, pp 499–558. <https://doi.org/10.1016/B978-0-08-095975-7.00813-5>
7. Bhandari N, Lal D, Rama D (1966) Stratospheric circulation studies based on natural and artificial radioactive tracer elements. *Tellus Ser A* 18(2–3):391–406. <https://doi.org/10.3402/tellusa.v18i2-3.9390>
8. Bhandari N, Lal D, Rama (1970) Vertical structure of the troposphere as revealed by radioactive tracer studies. *J Geophys Res* 75(15):2974–2980. <https://doi.org/10.1029/JC075i015p02974>
9. Benitez-Nelson CR, Buesseler KO (1999) Phosphorus 32, phosphorus 33, beryllium 7, and lead 210: atmospheric fluxes and utility in tracing stratosphere/troposphere exchange. *J Geophys Res* 104(D9):11745–11754. <https://doi.org/10.1029/1998JD100101>
10. Lujanas V, Lujanienė G (2007) Application of cosmogenic radionuclides in ozone tracer studies. *J Radioanal Nucl Chem* 274(2):287–291. <https://doi.org/10.1007/s10967-007-1113-1>
11. Benitez-Nelson CR, Buesseler KO (1998) Measurement of cosmogenic  $^{32}\text{P}$  and  $^{33}\text{P}$  activities in rainwater and seawater. *Anal Chem* 70(1):64–72. <https://doi.org/10.1021/ac9707500>
12. Van Mooy BAS, Krupke A, Dyhrman ST, Fredricks HF, Frischkorn KR, Ossolinski JE, Repeta DJ, Rouco M, Seewald JD, Sylva SP (2015) Major role of planktonic phosphate reduction in the marine phosphorus redox cycle. *Science* 348(6236):783–785. <https://doi.org/10.1126/science.aaa8181>
13. Benitez-Nelson C (2015) The missing link in oceanic phosphorus cycling? *Science* 348(6236):759–760. <https://doi.org/10.1126/science.aab2801>
14. Lal D, Chung Y, Platt T, Lee T (1988) Twin cosmogenic radiotracer studies of phosphorus recycling and chemical fluxes in the upper ocean. *Limnol Oceanogr* 33(6 part 2):1559–1567. <https://doi.org/10.4319/lo.1988.33.6part2.1559>
15. Lal D, Lee T (1988) Cosmogenic  $^{32}\text{P}$  and  $^{33}\text{P}$  used as tracers to study phosphorus recycling in the upper ocean. *Nature* 333(6175):752–754. <https://doi.org/10.1038/333752a0>
16. Lee T, Barg E, Lal D (1991) Studies of vertical mixing in the Southern California Bight with cosmogenic radionuclides  $^{32}\text{P}$  and  $^7\text{Be}$ . *Limnol Oceanogr* 36(5):1044–1052. <https://doi.org/10.4319/lo.1991.36.5.1044>
17. Lee T, Lal D (1992) Techniques for extraction of dissolved inorganic and organic phosphorus from large volumes of sea water. *Anal Chim Acta* 260(1):113–121. [https://doi.org/10.1016/0003-2670\(92\)80134-S](https://doi.org/10.1016/0003-2670(92)80134-S)
18. Waser NA, Fleer AP, Hammar TR, Buesseler KO, Bacon MP (1994) Determination of natural  $^{32}\text{P}$  and  $^{33}\text{P}$  in rainwater, marine particles and plankton by low-level beta counting. *Nucl Instrum Methods Phys Res Sect A* 338(2–3):560–567. [https://doi.org/10.1016/0168-9002\(94\)91342-0](https://doi.org/10.1016/0168-9002(94)91342-0)
19. Waser NAD, Bacon MP (1994) Cosmic ray produced  $^{32}\text{P}$  and  $^{33}\text{P}$  in Cl, S and K at mountain altitude and calculation of oceanic production rates. *Geophys Res Lett* 21(11):991–994. <https://doi.org/10.1029/94GL00878>
20. Waser NAD, Bacon MP (1995) Wet deposition fluxes of cosmogenic  $^{32}\text{P}$  and  $^{33}\text{P}$  and variations in the  $^{33}\text{P}/^{32}\text{P}$  ratios at Bermuda. *Earth Planet Sci Lett* 133(1–2):71–80. [https://doi.org/10.1016/0012-821X\(95\)00073-L](https://doi.org/10.1016/0012-821X(95)00073-L)
21. Waser NAD, Bacon MP, Michaels AF (1996) Natural activities of  $^{32}\text{P}$  and  $^{33}\text{P}$  and the ratio in suspended particulate matter and plankton in the Sargasso Sea. *Deep Sea Res Part II* 43(2–3):421–436. [https://doi.org/10.1016/0967-0645\(95\)00092-5](https://doi.org/10.1016/0967-0645(95)00092-5)
22. Benitez-Nelson CR, Buesseler KO (1999) Variability of inorganic and organic phosphorus turnover rates in the coastal ocean. *Nature* 398(6727):502–505. <https://doi.org/10.1038/19061>
23. Chen M, Yang Z, Zhang L, Qiu Y, Ma Q, Huang Y (2013) Determination of cosmogenic  $^{32}\text{P}$  and  $^{33}\text{P}$  in environmental samples. *Acta Oceanol Sin* 32(6):18–25. <https://doi.org/10.1007/s13131-013-0305-5>
24. Nakanishi T, Kusakabe M, Aono T, Yamada M (2009) Simultaneous measurements of cosmogenic radionuclides  $^{32}\text{P}$ ,  $^{33}\text{P}$  and  $^7\text{Be}$  in dissolved and particulate forms in the upper ocean. *J Radioanal Nucl Chem* 279(3):769–776. <https://doi.org/10.1007/s10967-008-7374-5>
25. Vértes A, Nagy S, Klencsár Z, Lovas RG, Rösch F (eds) (2011) *Handbook of nuclear chemistry*. Springer, New York. <https://doi.org/10.1007/978-1-4419-0720-225>

26. Papastefanou C, Ioannidou A (1994) Aerodynamic size of  $^7\text{Be}$  in ambient aerosols. *J Environ Radioact* 26:273–281. [https://doi.org/10.1016/0265-931X\(94\)00011-K](https://doi.org/10.1016/0265-931X(94)00011-K)
27. Koch D, Jacob D, Graustein W (1996) Vertical transport of tropospheric aerosols as indicated by  $^7\text{Be}$  and  $^{210}\text{Pb}$  in a chemical tracer model. *J Geophys Res* 101(D13):18651–18666. <https://doi.org/10.1029/96JD01176>
28. Usoskin IG, Fieldy CV, Schmidy GA, Leppanenz A-P, Aldahanx A, Kovaltsov GA, Possnert G, Ungar RK (2009) Cosmogenic isotope  $^7\text{Be}$  as a tracer for air mass dynamics. In: Proceedings of the 31st ICRC, ŁÓDŹ
29. Kadko D, Olson D (1996) Beryllium-7 as a tracer of surface water subduction and mixed-layer history. *Deep-Sea Res* 43(2):89–116. [https://doi.org/10.1016/0967-0637\(96\)00011-8](https://doi.org/10.1016/0967-0637(96)00011-8)
30. Tanaka N, Turekian KK (1995) Determination of the dry deposition flux of  $\text{SO}_2$  using cosmogenic  $^{35}\text{S}$  and  $^7\text{Be}$  measurements. *J Geophys Res* 100(D2):2841–2848. <https://doi.org/10.1029/94JD02305>
31. Mann M, Beer J, Steinhilber F, Abreu JA, Christl M, Kubik PW (2011) Variations in the depositional fluxes of cosmogenic beryllium on short time scales. *Atmos Environ* 45:2836–2841. <https://doi.org/10.1016/j.atmosenv.2011.03.005>
32. Egorov V, Gulin S, Polikarpov G, Osvath I (2010) Black sea: radionuclides. *Encycl Inorg Chem*. <https://doi.org/10.1002/0470862106.ia761>
33. Baskaran M, Coleman CH, Santschi PH (1993) Atmospheric depositional fluxes of  $^7\text{Be}$  and  $^{210}\text{Pb}$  at Galveston and College Station, Texas. *J Geophys Res* 98(D11):20555–20571. <https://doi.org/10.1029/93JD02182>
34. Huh C-A, Su C-C, Shiau L-J (2006) Factors controlling temporal and spatial variations of atmospheric deposition of  $^7\text{Be}$  and  $^{210}\text{Pb}$  in northern Taiwan. *J Geophys Res* 111(D16):304. <https://doi.org/10.1029/2006JD007180>
35. Feely HW, Larsen RJ, Sanderson CG (1989) Factors that cause seasonal variations in Be-7 concentrations in surface air. *J Environ Radioact* 9:223–249
36. Danielsen EF (1968) Stratospheric–tropospheric exchange based on radioactivity, ozone and potential vorticity. *J Atmos Sci* 25:502–518
37. Vaughan G (1988) Stratosphere–troposphere exchange of ozone. In: Isaksen ISA (ed) *Tropospheric ozone*. Reidel Publishing, Dordrecht, pp 125–135
38. Vaughan G, Price JD (1989) Ozone transport into the troposphere in a cut-off low event. In: Bojkov RD, Fabian P (eds) *Ozone in the atmosphere*. Deepak Publishing, Hampton, pp 415–418
39. Ancellet G, Beekmann M, Papayannis A (1994) Impact of a cut-off low development on downward transport of ozone in the troposphere. *J Geophys Res* 99(D2):3451–3468
40. Baskaran M, Coleman CH, Santschi PH (1993) Atmospheric deposition fluxes of Be-7 and Pb-210 at Galveston and College station, Texas. *J Geophys Res* 98:20555–20571
41. Brost RA, Feichter J, Heimann M (1991) Three-dimensional simulation of  $^7\text{Be}$  in a global climate model. *J Geophys Res* 96(D12):22423–22445
42. Cannizzaro F, Greco G, Ranelli M, Spitale MC, Tomarchio E (2004) Concentration measurements of  $^7\text{Be}$  at ground level air at Palermo, Italy- comparison with solar activity over a period of 21 years. *J Environ Radioact* 72:259–271
43. Arkian F, Salahinejad M, Bidokhti AA, Meshkatee A (2008) Analysis of gross alpha, gross beta activities and beryllium-7 concentrations in surface air: their variations and statistical prediction model. *Environ Monit Assess* 140(1–3):325–330
44. Charlot G (1961) *Les methodes de la chimie analytique*. Quatrième édition entièrement refondue. Masson et Cie, Paris, p 1204
45. Grasshoff K, Ehrhardt M, Kremling K, Anderson LG (1999) *Methods of seawater analysis*. 3rd, completely rev. and extended ed. Wiley, Weinheim, p 600
46. Jungck MHA, Andrey J-L, Froidevaux P (2009) Determination of radionuclide levels in rainwater using ion exchange resin and  $\gamma$ -spectrometry. *J Environ Radioact* 100(4):361–365. <https://doi.org/10.1016/j.jenvrad.2009.01.006>
47. Goel PS, Narasappaya N, Prabhakara C, Rama Thor, Zutshi PK (1959) Study of cosmic ray produced short-lived  $\text{P}^{32}$ ,  $\text{P}^{33}$ ,  $\text{Be}^7$ , and  $\text{S}^{35}$  in tropical latitudes. *Tellusa* 11(1):91–100. <https://doi.org/10.3402/tellusa.v11i1.9278>
48. Papastefanou C, Ioannidou A (1991) Depositional fluxes and other physical characteristic of atmospheric beryllium-7 in the temperate zones ( $40^\circ\text{N}$ ) with a dry (precipitation-free) climate. *Atmos Environ Part A* 25(10):2335–2343. [https://doi.org/10.1016/0960-1686\(91\)90108-J](https://doi.org/10.1016/0960-1686(91)90108-J)
49. Lozano RL, San Miguel EG, Bolívar JP, Baskaran M (2011) Depositional fluxes and concentrations of  $^7\text{Be}$  and  $^{210}\text{Pb}$  in bulk precipitation and aerosols at the interface of Atlantic and Mediterranean coasts in Spain. *J Geophys Res* 116:D18213. <https://doi.org/10.1029/2011JD015675>
50. Pham MK, Povinec PP, Nies H, Betti M (2013) Dry and wet deposition of  $^7\text{Be}$ ,  $^{210}\text{Pb}$  and  $^{137}\text{Cs}$  in Monaco air during 1998–2010: seasonal variations of deposition fluxes. *J Environ Radioact* 120:45–57. <https://doi.org/10.1016/j.jenvrad.2012.12.007>
51. Lal D (1959) Cosmic ray produced radioisotopes for studying the general circulation in the atmosphere. *Indian J Meteorol Geophys* 10:147–154
52. Rama M, Honda M (1961) Natural radioactivity in the atmosphere. *J Geophys Res* 66(10):3227–3231. <https://doi.org/10.1029/JZ066i010p03227>